Molecules and Cells

Moieties of Complement iC3b Recognized by the I-domain of Integrin αXβ2

Jeongsuk Choi[1], Dolgorsuren Buyannemekh[1], and Sang-Uk Nham[2],*

[1]Department of Biology, Kangwon National University, Chuncheon 24341, Korea, [2]Division of Science Education, Kangwon National University, Chuncheon 24341, Korea
*Correspondence: sunham@kangwon.ac.kr
https://doi.org/10.14348/molcells.2020.0197
www.molcells.org

Complement fragment iC3b serves as a major opsonin for facilitating phagocytosis via its interaction with complement receptors CR3 and CR4, also known by their leukocyte integrin family names, αMβ2 and αXβ2, respectively. Although there is general agreement that iC3b binds to the αM and αX I-domains of the respective β2-integrins, much less is known regarding the regions of iC3b contributing to the αX I-domain binding. In this study, using recombinant αX I-domain, as well as recombinant fragments of iC3b as candidate binding partners, we have identified two distinct binding moieties of iC3b for the αX I-domain. They are the C3 convertase-generated N-terminal segment of the C3b α'-chain (α'NT) and the factor I cleavage-generated N-terminal segment in the CUBf region of α-chain. Additionally, we have found that the CUBf segment is a novel binding moiety of iC3b for the αM I-domain. The CUBf segment shows about a 2-fold higher binding activity than the α'NT for αX I-domain. We also have shown the involvement of crucial acidic residues on the iC3b side of the interface and basic residues on the I-domain side.

Keywords: binding sites, complement, iC3b, I-domain, integrins, protein-protein interactions, αMβ2, αXβ2

INTRODUCTION

The complement system plays an essential role in host de-fense against pathogenic microorganisms, both by facilitating their clearance via phagocytic cells and by providing a link between the innate and adaptive arms of the immune system (Carroll, 2004; Ricklin et al., 2010). Both of these functions are mediated via specific cellular receptor interactions with complement C3 proteolytic split products that covalently decorate the surface of the microorganism. Regardless of the initiating complement pathway, proteolytic cleavage of native C3 by a foreign target-associated C3 convertase enzyme results in several of the domains of the large (~190 kDa) cleavage product, C3b undergoing a major conformational rearrangement. One effect of this is to expose the previously buried, but now highly reactive intramolecular thioester bond in the thioester domain (TED) of C3b such that a portion of the molecules transacylate to hydroxyl groups on the target surface, thus anchoring the C3b molecule via an ester linkage (Gros et al., 2008). Another effect of the conformational rearrangement is to reveal cryptic sites such as the N-terminal segment of the C3b α'-chain (α'NT), that permit C3b to in-teract with other soluble and membrane-associated comple-ment family members involved in both the propagation and regulation of the complement pathways, as well as in the clearance of C3b-opsonized targets (Fig. 1A).

C3b undergoes subsequent cleavages by the complement regulatory enzyme factor I (FI), which excises a C3f segment from the CUB (complement C1r/C1s, sea urchin EGF, and bone morphogenic protein 1 related domain) domain of the C3b α-chain, resulting the iC3b having a new N-terminus in

what is structurally denoted as the CUBf segment (Janssen et al., 2005). Subsequently, FI mediates a third cleavage within the CUB domain, releasing the major C3c portion of the molecule into the fluid phase, but leaving the C3dg fragment still covalently attached to the target. A non-complement protease can remove C3g from the N-terminus of C3dg to generate a C3d fragment. This proteolytic limit fragment corresponds closely in its boundaries to those of the structurally-defined TED (Fig. 1A).

Among the complement C3-split products, iC3b serves as the major opsonin for facilitating phagocytosis of foreign pathogens by leukocytes and it binds to several complement receptors (CR) such as CR2, CR3, CR4, and CRIg. The CR3 and CR4, the two family members of β2 integrin, are also
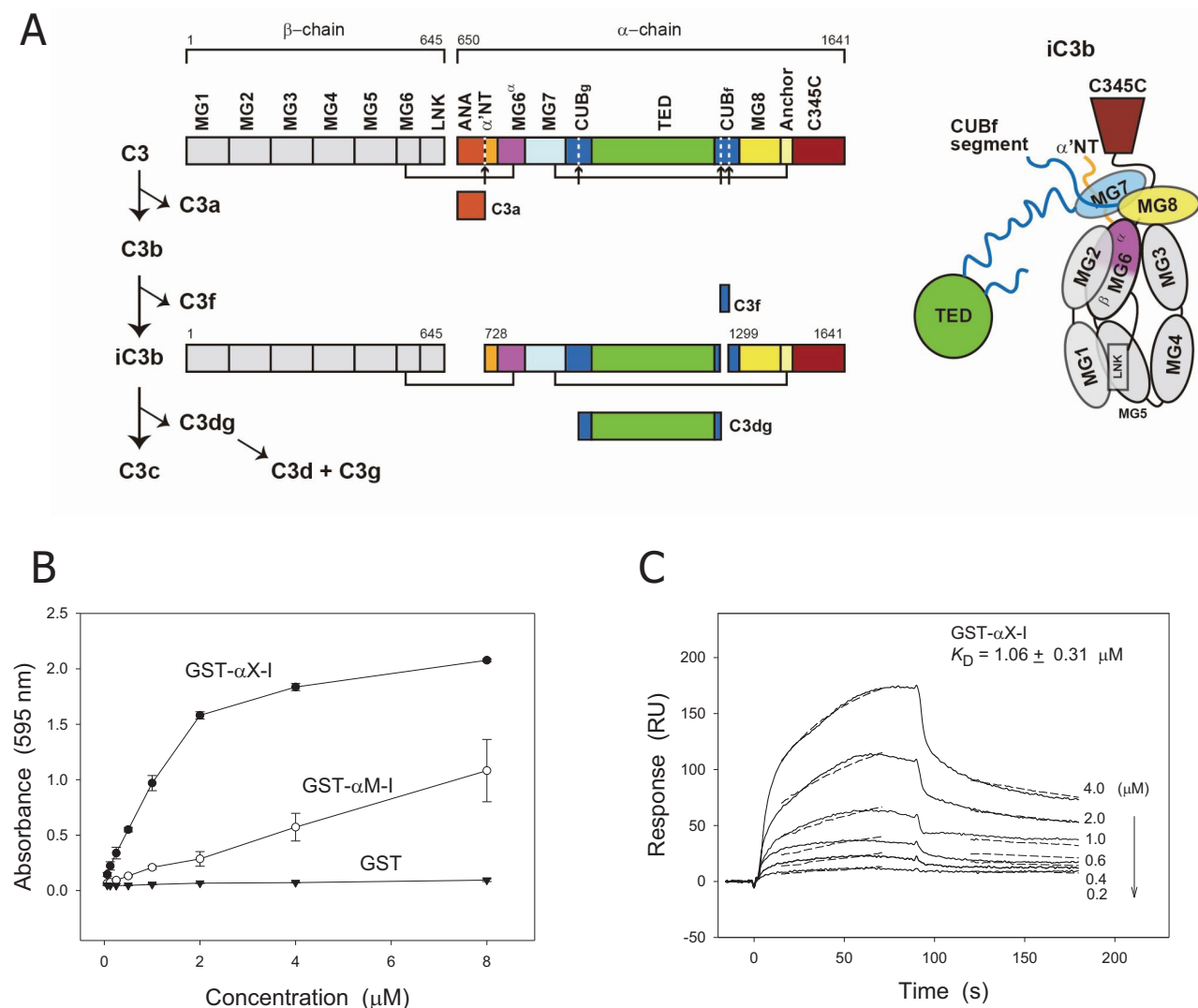

Fig. 1. A schematic representation of the structure of iC3b molecule and analyses of GST-αX I-domain binding to iC3b by an ELISA-based assay or by an SPR analysis. (A) The domain sequence and proteolytic cleavage of native C3 to iC3b, and a schematic representation of the structure of iC3b. The β-(residues 1-645) and α-chains (residues 650-1641) of C3 protein are covalently linked through a disulfide bond between MG6 domains. A series of proteolytic cleavages generate several C3 split products such as C3b, iC3b, and C3c, and arrows indicate proteolytic cleavage sites. The cartoon of iC3b shows the simplified structure of the molecule with several domains and exposed two N-termini, an α'NT and a CUBf segment. MG, macroglobulin domain; CUB, complement C1r/C1s, sea urchin EGF, and bone morphogenic protein 1 related domain; TED, thioester domain; C345C, C-terminal domain of the C3/C4/C5 protein family. Adapted from previous reports (Gros et al., 2008; Janssen et al., 2005). (B) An ELISA-type binding assay was carried out with various concentrations of the GST-αX I-domain and the GST-αM I-domain being offered to immobilized iC3b on microtiter plate wells. Data is shown as mean ± SD (n = 4). (C) An SPR kinetic analysis of αX I-domain binding to iC3b. Various concentrations of the GST-αX I-domain were injected to flow over the immobilized iC3b (4000 RU) on a CM5 chip. The responses (solid line) from the injection of various concentrations of the I-domain are overlaid with the fit of a 1:1 interaction model (dotted line) in the region of kinetic analysis for association and dissociation rate constants. The dissociation constant (K_D) of the αX I-domain binding to iC3b was calculated by three independent SPR experiments and shown as a mean ± SD.

known by their integrin nomenclature as αMβ2 and αXβ2, respectively (Helmy et al., 2006; Janssen and Gros, 2007; Ross and Medof, 1985).

The β2 integrins, consist of a common β subunit (β2, CD18) and specific α subunits such as αL, αD, αM, and αX. The αMβ2 and αXβ2 integrins bind to a largely overlapping array of ligands, reflecting a 63% sequence identity between their α subunits. These include, but are not limited to iC3b, intercellular adhesion molecule-1 (ICAM-1), fibrinogen, and heparin (Choi et al., 2010; Luo et al., 2007; Plow et al., 2000). The αMβ2 and αXβ2 integrins also have a partially overlapping leukocyte distribution profile, both being present on circulating monocytes, macrophages and natural killer (NK) cells. Whereas αMβ2 is the dominant β2 integrin on neutrophils, αXβ2 is the major β2 integrin on dendritic cells and on tissue-resident macrophages (Luo et al., 2007; Myones et al., 1988). All of the β2 integrin α subunits possess a primary ligand binding domain, namely the I-domain, which consists of approximately 200 amino acids and forms an α/β Rossmann-fold type of three dimensional structure with seven α helices and six β sheets (Lee et al., 1995; Vorup-Jensen et al., 2003). There is a metal ion dependent adhesion site (MIDAS) on the "top" surface of the I-domains of the β2 integrins and this reflects their requirement of divalent cations (physiologically Mg^{2+}) for ligand binding (Arnaout et al., 2005). In addition to the metal ion requirement, β2 integrins need to undergo an activation process to bind their ligands. This process brings about major conformational changes in the intact molecule so as to both sterically unmask, and allosterically render competent their ligand binding sites (Luo et al., 2007).

Many studies point to the critical role of the I-domain of αMβ2 in the binding of iC3b (Diamond et al., 1993; Michishita et al., 1993; Ueda et al., 1994), and the binding site(s) within iC3b for the αMβ2 are now relatively well defined. One potential site in iC3b resides within the N-terminal segment of the α'-chain (α'NT), where mutations of a cluster of acidic residues affect the interactions of C3b with CR1, and of iC3b with αMβ2 (Taniguchi-Sidle and Isenman, 1994). There were also several reports in the literature suggesting that C3dg, or its proteolytic limit fragment C3d, may contribute in part to the binding interaction with αMβ2. Specifically, it was found that human monocytes cultured on glass would rosette with sheep red cells bearing relatively high numbers of human C3d molecules, that these rosettes were divalent cation-dependent, and were partially inhibited by anti-Mo1, the latter being a monoclonal antibody directed against αMβ2 (Gaither et al., 1987; Inada et al.,1983). A more contemporary report employing surface plasmon resonance (SPR) and isothermal titration calorimetry binding studies, as well as X-ray crystallographic structural studies has confirmed that C3d does indeed comprise a major binding site within iC3b for the I-domain of αMβ2 and that Asp1247 in C3d is essential for the αM I-domain interaction as its side chain carboxylate group coordinates the Mg^{2+} ion of the MIDAS site (Bajic et al., 2013). Negative-stain electron microscopy (EM) of an iC3b complexed to intact αMβ2 also showed that the αM I-domain binds the TED of the iC3b (Xu et al., 2017).

In contrast to the information about the binding site(s)

within iC3b for the αMβ2, the regions of iC3b contributing to the interaction with the β2 integrin are less well known. A negative-stain EM study of iC3b or C3c liganded to an active form of αX I-domain or to an intact αXβ2 complex showed that the I-domain of αXβ2 contacted iC3b at one of two sites. The dominantly-observed site was at the junction between the MG3 and MG4 domains on the β-chain ring of the iC3b molecule. However, in less frequently observed images, the αX I-domain was bound near the C345C domain of iC3b (Xu et al., 2017). The authors also found that the interface of MG3 and MG4 of the iC3b serves as a binding site only for αXβ2, but not for αMβ2. They, however, could not clearly define the nature of the secondary binding sites near the C345C knob.

In order to define more moieties of iC3b involved in the binding to CR4/αXβ2, we used a recombinant αX I-domain to probe the involvement of several candidate binding sites within iC3b. Our results indicate the involvement of both an α'NT segment and a site near the FI cleavage-generated N-terminus of the residual CUBf segment in the C3 α-chain for αX I-domain binding. In addition, we provide information regarding critical amino acid residues within these sites for the recognition of the αX and αM I-domains of β2 integrins.

MATERIALS AND METHODS

Peptides and proteins
Two peptides derived from the N-terminus of the C3 α'-chain (DEDIIAEE, SRSEFPES) and two peptides from the amino terminus of CUBf (SEETKENE, TAEGKGQG) were synthesized by the Peptron (Korea).

Construction of recombinant plasmids
For production of the GST-αX I-domain and the GST-αM I-domain, two expression plasmids, pEXCD11cI and pEX-CD11bI, were used as previously reported (Lee et al., 2007). Expression plasmids, pETαXI and pETαMI, were constructed to express His₆ tag sequences at the N-termini of the αX I-domain (P127 to K313) and αM I-domain (P129 to K315), respectively. A PCR-amplified cDNA fragment encoding an αX I-domain was cloned in frame into the BamHI and XhoI sites of vector pET28c for the construction of pETαXI. Similarly, a PCR-amplified cDNA segment encoding the αM I-domain was inserted into the BamHI and NotI sites of vector pET28a for pETαMI. For the production of αX I-domain mutants, several previously described mutant bacterial cDNA expression clones were used (Lee et al., 2007).

N-terminal and C-terminal GST fusions of the N-terminal α-chain segment of C3b, and of the new N-terminal peptide within the CUBf segment generated when C3b is cleaved by FI, were created by appropriate PCR reactions with the wild type human C3 cDNA plasmid pSVC3 (Taniguchi-Sidle and Isenman, 1992) and cloning into GST expression vectors as described further below. The amplified cDNAs encoded the amino terminus of α'NT (N728-V753, mature C3 numbering used throughout to designate polypeptide boundaries) and the amino terminus of a CUBf segment (S1299-K1238). In this study, these peptides were referred to as αNTN and αCUN. These DNA fragments were ligated into pENTR/D-TO-

PO vector (Invitrogen, USA) according to manufacturer's instructions. After sequence analysis to verify their authenticity, cDNA for αNTN and αCUN were inserted into a pDEST15 vector using homologous recombination (Invitrogen). The resulting expression vectors, namely pDGαNTN and pDGαCUN, which respectively express αNTN and αCUN at the C-terminus of GST, were introduced into *Escherichia coli* BL21(DE3)pLysS for recombinant protein production.

To express αCUN at the amino terminus of GST, cDNA encoding αCUN was amplified with a primer set providing a translation start codon. This cDNA was ligated into pENTR/SD-TOPO, a PCR product cloning vector providing a Shine–Dalgarno (SD) sequence 5' upstream of the cDNA. The αCUN cDNA containing the SD sequence was subsequently inserted into pDEST24 to form the expression plasmid pDEαCUN9.

To obtain mutant proteins derived from αNTN and αCUN, site-directed mutagenesis was carried out on pDGαNTN and pDGαCUN by using a QuikChange™ mutagenesis kit (Stratagene, USA). All constructs were verified by DNA sequencing.

Production of glutathione S-transferase fusion proteins

The *E. coli* strain BL21 was the host strain for all pGEX and pDEST15 vector-derived plasmids expressing the I-domains of β2 integrin, and the αNTN and αCUN of iC3b. Bacterial cells (BL21) transformed by expression plasmids were incubated to a log phase of growth (A_{600} = 0.3-0.5) in a 400 ml volume of LB-ampicillin and then treated with 0.5 mM isopropyl-thio-β-D-galactoside (IPTG) for 4 to 6 h. Harvested bacterial cell pellets were resuspended in 10 ml of 20 mM phosphate buffer, pH 7.5, 150 mM NaCl (PBS) and then lysed in a high-pressure homogenizer (French press). Bacterial lysates diluted in 40 ml of PBS were incubated with Glutathione-Sepharose 4B resin (2 ml; GE Healthcare Bio-Science, USA) for 1 h with gentle shaking at 4°C. The resin bound with fusion proteins was washed with PBS containing 0.1% Triton × 100. GST fusion proteins were eluted by 10 mM of reduced glutathione in 20 mM Tris/HCl, pH 8.0 and dialyzed against PBS. After assessment of the homogeneity of the eluted protein by SDS-PAGE, the proteins were concentrated using Centricon spin concentrators (Millipore, USA). Each protein concentration was determined by a Bradford assay (Bio-Rad, USA).

Production of His tagged recombinant proteins

The *E. coli* strain BL21(DE3)pLysS was used to produce all the pET or pDEST24 vector-derived His-tagged proteins employed in this study. Bacterial cells hosting these expression plasmids were incubated in 400 ml of LB-ampicillin medium to a log phase of growth (A_{600} = 0.3-0.5) and then treated with 0.5 mM IPTG for 15 h. French press lysis of pelleted bacteria was as described above for the GST-fusion constructs. For purification of His-tagged proteins, bacterial cell lysates were diluted with 20 ml of PBS and were incubated with Ni-NTA Sepharose (2 ml; Qiagen, Germany) for 1 h with gentle shaking at 4°C. The resin was washed with PBS containing 0.1% Triton × 100 and His-tagged proteins were eluted with a buffer consisting of 50 mM sodium phosphate, 300 mM NaCl, and 250 mM imidazole. The eluted proteins were subsequently dialyzed against PBS.

Enzyme-linked immunosorbent assay (ELISA)-based binding assay

Ligand protein at a concentration of 10.0 μg/ml in PBS, pH 7.4, was added to wells on microtiter plates (Immulon, USA) and incubated overnight at 4°C. The plates were washed with PBS and blocked for 2 h with blocking buffer (PBS with 5% bovine serum albumin). Wells were then loaded with analyte protein (usually 100 μl) in binding medium (50 mM Tris/HCl, pH 7.4, 150 mM NaCl, 5% bovine serum albumin, 1 mM $MgCl_2$) and then incubated for 60 min. The plates were washed with PBS with 0.1% Triton × 100 and then mouse anti-GST antibody (1/2,000 dilution; BD Biosciences, USA), was loaded and incubated for 1 h. Following washing, the wells were incubated for 1 h with alkaline phosphatase-conjugated anti-mouse IgG. Following three more rounds of washing with PBS/0.1% Triton × 100, bound antibody conjugate was detected by the addition of an alkaline phosphatase substrate, BluePhos™ (KPL, USA). The color intensity of each well was measured at 595 nm (Bio-Rad microplate reader 550; Bio-Rad).

Characterization of binding by SPR analysis

SPR experiments were performed on a Biacore X (GE Healthcare Bio-Science). All experiments were carried out at 25°C, and generally analytes were diluted with HBS-Mg buffer (150 mM NaCl, 10 mM HEPES, pH 7.4, 1 mM $MgCl_2$). GST-αX I, His$_6$-αX I, or iC3b proteins were immobilized on respective carboxyl-methyl dextran chips (CM5) according to the manufacturer's instructions. For each chip, an activated and blocked flow channel without any ligands was used as a reference to correct for bulk effects and nonspecific binding. Analytes were injected for 90 s for association, and dissociation data was collected for 90 s. Removal of bound protein was with 20 mM Tris/HCl, 0.3 M NaCl, 20 mM EDTA, pH 8.0, followed by re-equilibration with HBS-Mg prior to the next injection of analyte.

For the kinetic analysis, analytes were injected at the speed of 30 μl/min and dissociation constant (K_D) was calculated by curve fitting of association and dissociation phases by using the 1:1 Langmuir binding model of the BIAevaluation 3.0 software (GE Healthcare Bio-Science).

For analyzing the relative binding activities of analytes, samples were injected at the speed of 20 μl/min and the binding levels of the analytes were calculated from the steady-state plateau regions of the association phase of each sensogram.

RESULTS

Binding of αX I-domain to iC3b

As a first step to analyze the moieties of iC3b recognized by the I-domains of the αXβ2, we analyzed the binding affinity of these recombinant I-domains for iC3b by using an ELISA-based binding assay and an SPR kinetic analysis. The results of the ELISA-based assay show that αX I-domain binds at a considerably higher level to iC3b than does the αM I-domain (Fig. 1B). This data suggests an apparent dissociation constant (K_D) of approximately 1 μM for αX I-domain binding to iC3b, whereas the apparent K_D for the interaction with the

αM I-domain, although obviously higher, could not be confidently determined because even at the highest concentration tested (8 μM) only about 50% of the anticipated saturation level had been achieved. From the kinetic analysis, the K_D of αX I-domain binding to iC3b was calculated to be 1.06 μM, which is consistent with the ELISA-based binding data (Fig. 1C). As shown in the SPR sensogram, all binding curves (solid lines) generally fitted well to the Langmuir binding model (dotted lines), showing a good fit in the region of kinetic analysis for association and dissociation rate constants. These results suggest that as iC3b binding is stronger for the αX I-domain than for the αM I-domain, αXβ2 may play a more significant role than αMβ2 in the phagocytosis of opsonized pathogens, especially by tissue-resident macrophages, which in any case express more αXβ2 than αMβ2.

We next sought to identify important amino acid residues within the αX I-domain for iC3b binding. As our earlier studies had identified residues within the βDα5 loop of the αX

I-domain as being a major point of contact with two other αX I-domain ligands, specifically ICAM-1 and plasminogen (Choi et al., 2010; Gang et al., 2007), the binding interaction with iC3b was explored using a series of previously engineered charged residue mutants targeting the βDα5 loop of αX I-domain. The positions of the mutated residues within the βDα5 loop sequence are shown in Fig. 2A. Two negatively charged amino acids (D240 and D246) were excluded as point mutation targets because of their important roles in the structural stability of the I-domain. D240 is essential for metal ion binding and D246 is required for an internal hydrogen bond.

As shown in Fig. 2B, alanine substitution of positively charged residues on the loop (K242A and K243A) inhibits the binding activity of the αX I-domain significantly, whereas a mutation of a basic residue (K251A) on the adjacent α5 helix does not. By contrast, substitution of acidic residues on the loop enhances the I-domain binding activity (K243S/
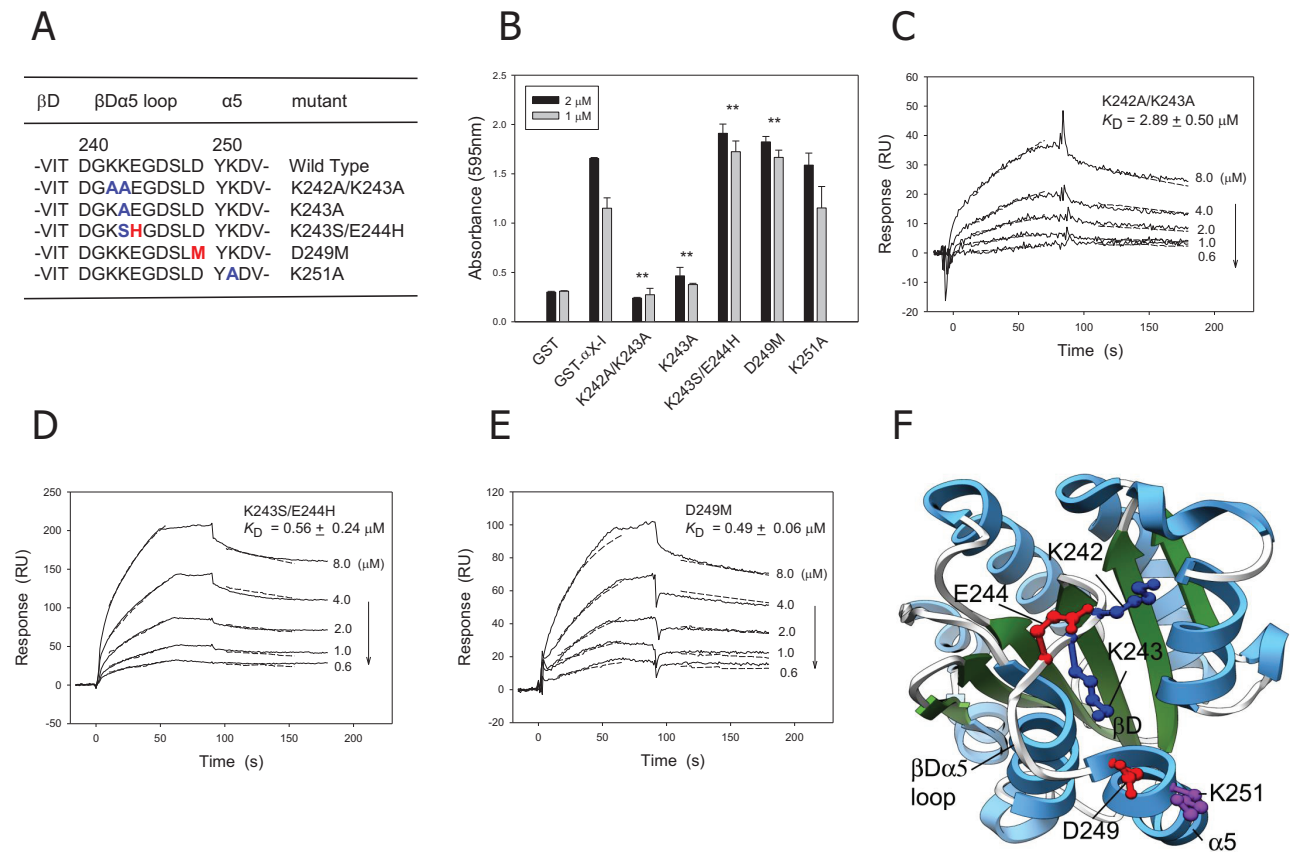

Fig. 2. Binding analyses of mutant αX I-domains to iC3b. (A) The position of substituted amino acids on the βDα5 loop, or α5 helix, in αX I-domain. (B) An ELISA-based binding assay of the mutant I-domains to immobilized iC3b. Results are expressed as mean ± SD (n = 4). **$P < 0.01$ (Student t-test) for the comparison of mutant to wild type αX I-domain binding. (C-E) SPR kinetic analyses of mutant GST-αX I-domains to immobilized iC3b (4000 RU). The dissociation constant (K_D) of each I-domain is shown as a mean ± SD (n = 3). (C) K242A/K234A, (D) K243S/E244H, (E) D249M. (F) A 3D structure of the αX I-domain in ribbon representation (PDB 1N3Y), (Vorup-Jensen et al., 2003) showing residues important for iC3b binding. The structure was drawn using the UCSF Chimera computer program (Pettersen et al., 2004). Positively charged residues important for iC3b binding are shown as blue (K242 and K243), whereas negatively charged residues playing no direct binding role are depicted as red (E244 and D249). K251, depicted in purple, represents a residue not implicated through mutation as being in contact with iC3b, even though it is positively charged. Also denoted are the α5 helix, the βD sheet and the βDα5 connecting loop.

E244H and D249M). In the case of the K243S/E244H double mutant, the introduction of the partially positively-charged histidine appears to rescue the defect caused by the loss of the positive charge at K243 when that substitution is present on its own. In addition to an ELISA-based binding assay, we measured the binding affinity of the mutant I-domains via an SPR kinetic analysis. As shown in Fig. 2C, the dissociation constant of the I-domain with positive amino acid substitution (K242A/K243A) is calculated as 2.89 μM which is about three times higher than that of the wild type I-domain, sug-
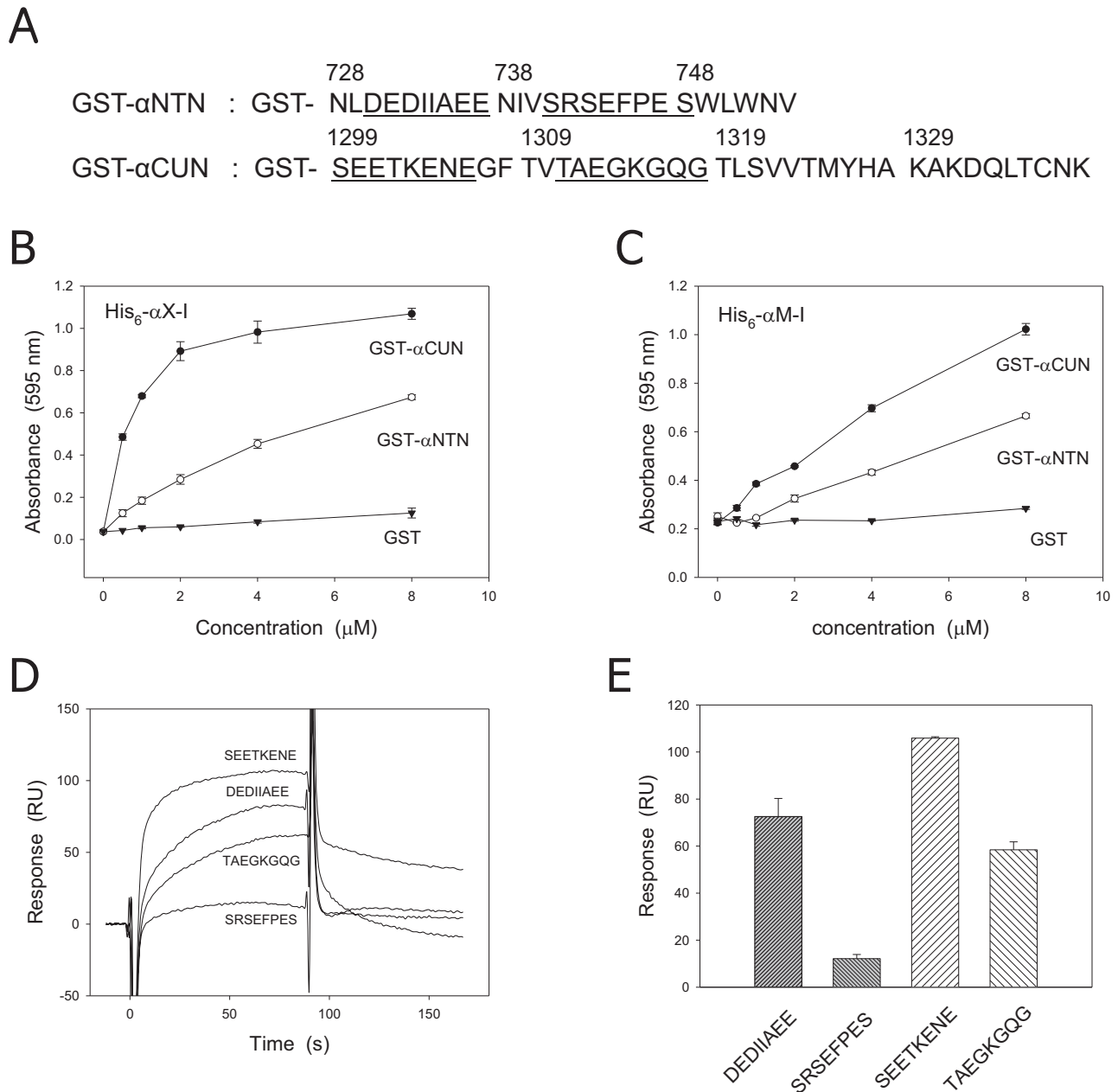
A

		728	738	748
GST-αNTN	: GST-	NL<u>DEDIIAEE</u>	NIV<u>SRSEFPE</u>	SWLWNV

		1299	1309	1319	1329
GST-αCUN	: GST-	<u>SEETKENE</u>GF	TV<u>TAEGKGQG</u>	TLSVVTMYHA	KAKDQLTCNK

Fig. 3. Binding analyses of αX and αM I-domains to the fragments derived from the two N-termini of C3 α-chain in iC3b. (A) Amino acid sequence of the iC3b-derived polypeptide segments in GST-αNTN and GST-αCUN. GST-αNTN and GST-αCUN are the GST fused peptides derived from the N-terminus of α'NT of iC3b and the CUBf segment, respectively. In these constructs, GST is fused to the amino terminal side of the peptides. Underbars represent the peptides (8 amino acids) used for binding to the αX I-domain. (B and C) ELISA-based binding assays of GST-αNTN and GST-αCUN to αX and αM I-domains. Various concentrations of GST-αNTN or GST-αCUN were loaded onto microtiter plate wells coated by His$_6$-αX I-domain (B) or His$_6$-αM I-domain (C). (D) SPR sensograms showing the binding activities of the peptides derived from the sequence of αNTN or αCUN to αX I-domain. Each peptide (1 mM) was injected to flow over the immobilized GST-αX I-domain (2000 RU) at the flow rate of 20 μl/min. (E) Comparison of the steady-state plateau binding levels of the peptides derived from the αNTN and the αCUN to αX I-domain. Data is shown as mean ± SD (n = 3).

gesting the substitution of positive amino acid lowers the binding affinity of the I-domain for iC3b. On the other hand, those of I-domains with substitution of acidic amino acids, K243S/E244H and D249M, were measured as 0.56 μM and 0.49 μM, respectively, which are about the half of that of the wild type I-domain, suggesting that the substitution of acidic amino acids elevates the binding affinity of the I-domain (Figs. 2D and 2E).

These results strongly suggest that the basic amino acids of the βDα5 loop are involved in direct contact with iC3b, whereas the acidic residues may mediate regulatory roles in an indirect way. By implication, the crucial roles of the basic residues K242 and K243 suggest that negatively charged amino acids in iC3b may be important for recognition of the αX I-domain. Fig. 2F shows the "top" surface of the αX I-domain crystal structure, indicating the residues implicated in iC3b binding. It is noteworthy that the βDα5 loop makes a groove running through the top surface and that the critical residues for iC3b binding (K242, K243) lie within this groove.

Binding of fragments derived from iC3b to the αXI-domain

There are two amino termini of the C3 α-chain in iC3b (Fig. 1A). One is the N-terminus of the α'NT segment, which is generated as a result of proteolytic cleavage of native C3 by C3 convertases. The other is at the N-terminus of the residual CUBf segment (S1299, mature C3 numbering) and is gen-

erated by factor I cleavage in the process of converting C3b to iC3b. As a next step to identify the interacting moieties of iC3b for the αX I-domain, the two N-termini of the C3 α-chain in iC3b were chosen as candidate sites for I-domain binding. A previous mutagenesis study had suggested that acidic amino acids within the α'NT segment contributed to the binding of iC3b to αMβ2 integrin (Taniguchi-Sidle and Isenman, 1994). Since the α'NT segment becomes surface accessible only following conversion of native C3 to C3b, and since its acidic residues contribute to the binding of several ligands of C3b (Becherer et al., 1992), it seemed likely that the N-terminus of CUBf generated in the process of converting C3b to iC3b would also have a change in its surface accessibility. Moreover, like α'NT, the N-terminus of CUBf is also relatively rich in acidic residues (Fig. 3A), and thus we hypothesized that these residues may interact with basic amino acid residues of the αX I-domain, possibly the ones that we had identified above as being important for iC3b binding.

To provide independent data regarding the role of the α'NT (N728-V753) in mediating binding to αMβ2 integrin I-domain, to test whether this segment also interacts with the αXβ2 integrin I-domain, and to test the hypothesis regarding the participation of the N-terminus of the CUBf polypeptide segment (S1299-K1338) in mediating binding of iC3b to the I-domain, the above delineated N-terminal polypeptide segments were expressed and purified from bacteria as GST fusion proteins. We refer to the GST fusions of the N-termini
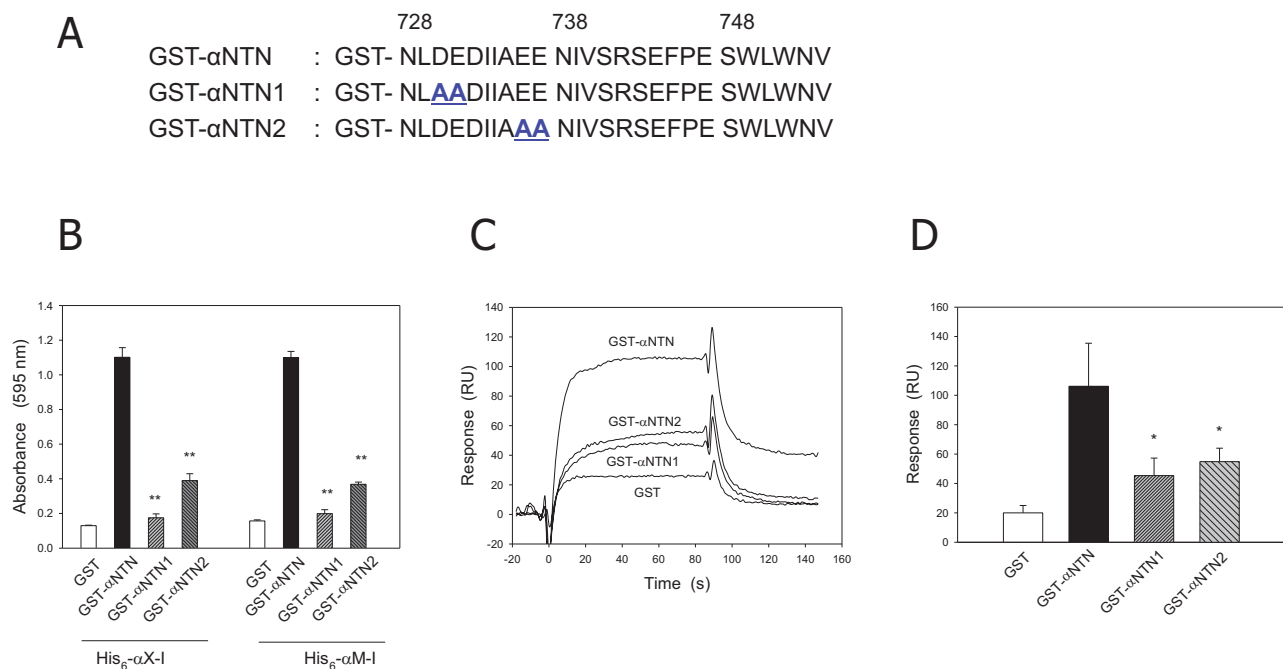

Fig. 4. Binding analyses of GST-αNTN and its mutants to the αX and αM I-domains. (A) Amino acid sequences of GST-αNTN and its alanine substitution mutants (acidic residues to alanine denoted in underbars). (B) An ELISA-based binding assay of GST-αNTN and its mutants to the His₆-tagged αX and αM I-domains coated on microtiterplate wells. Results for each of the GST-αNTN derivatives (1 μM) are shown as mean ± SD (n = 3). **$P < 0.01$ (Student t-test) for the comparison of mutant to wild type GST-αNTN binding. (C) SPR sensograms of wild type and mutant GST-αNTN (1 μM) binding to His₆-αX-I (3800 RU) immobilized on a CM5 chip. (D) Binding activities of the GST-αNTN mutants to αX I-domain. Each mutant binding level was measured from the steady-state plateau region of their respective SPR sensograms. Data is shown as mean ± SD (n = 3). *$P < 0.05$ (Student t-test).

of α'NT and of CUBf, the amino acid sequences which are shown in Fig. 3A, as GST-αNTN and GST-αCUN, respectively. As shown in Fig. 3B, these two GST fusion peptides were able to bind to His$_6$-αX I-domain coated on microtiter plates in a dose-dependent manner, whereas GST alone showed very minimal binding. The binding affinity of GST-αCUN appears to be several times higher than that of GST-αNTN. Since the N-terminus of the residual CUBf polypeptide segment has not been tested as a binding site of iC3b for αMβ2, we further carried out the ELISA-based binding assay with His$_6$-αM I-domain coated on microtiter plates. We found the GST-αCUN is also able to bind to αM I-domain, although the binding level of αM I-domain for the GST-αCUN is a little lower than that of the αX I-domain.

As a complementary approach, four peptides (8 amino acids each) derived from the sequences of αCUN and αNTN (Fig. 3A) were synthesized and tested at 1 mM concentration each for binding to the GST-αX I-domain immobilized via an SPR experiment. Typical binding sensograms of the four peptides to the I-domain and the binding levels of the peptides derived from SPR sensogram data are shown in Figs. 3D and 3E, respectively. It was found that peptides SEETKENE and TAEGKGQG, both being αCUN-derived, bind well to αX I-do-

main. For the αNTN peptides, whereas DEDIIAEE bound well, the more C-terminal peptide SRSEFPES showed little binding.

The role of acidic amino acids of αNTN in αXI-domain binding

Within the context of intact iC3b binding to αMβ2 on activated neutrophils, the mutation to alanine of the paired acidic residues E736 and E737, and to a lesser extent D730 and E731, resulted in substantially impaired binding (Taniguchi-Sidle and Isenman, 1994). The same mutations were introduced into the GST fusion peptides of αNTN (nomenclature key in Fig. 4A) and the binding of the mutant fusion peptides to the αX I-domain or the αM I-domain was assessed first in the ELISA-based binding assay. As shown in Fig. 4B, it can be seen that the loss of either of the paired acidic residues resulted in a major loss in binding activity to both of the I-domains. The αX I-domain bindings were confirmed via SPR analyses. As shown in Fig. 4C (typical sensograms of GST-αNTN and its mutant derivatives binding to the αX I-domain) and Fig. 4D (steady-state plateau binding levels of GST-αNTN and its mutant proteins to the αX I-domain), alanine substitution of the acidic amino acids inhibits αNTN binding to the αX I-domain. Taken together, these experiments employing α'NT fusion
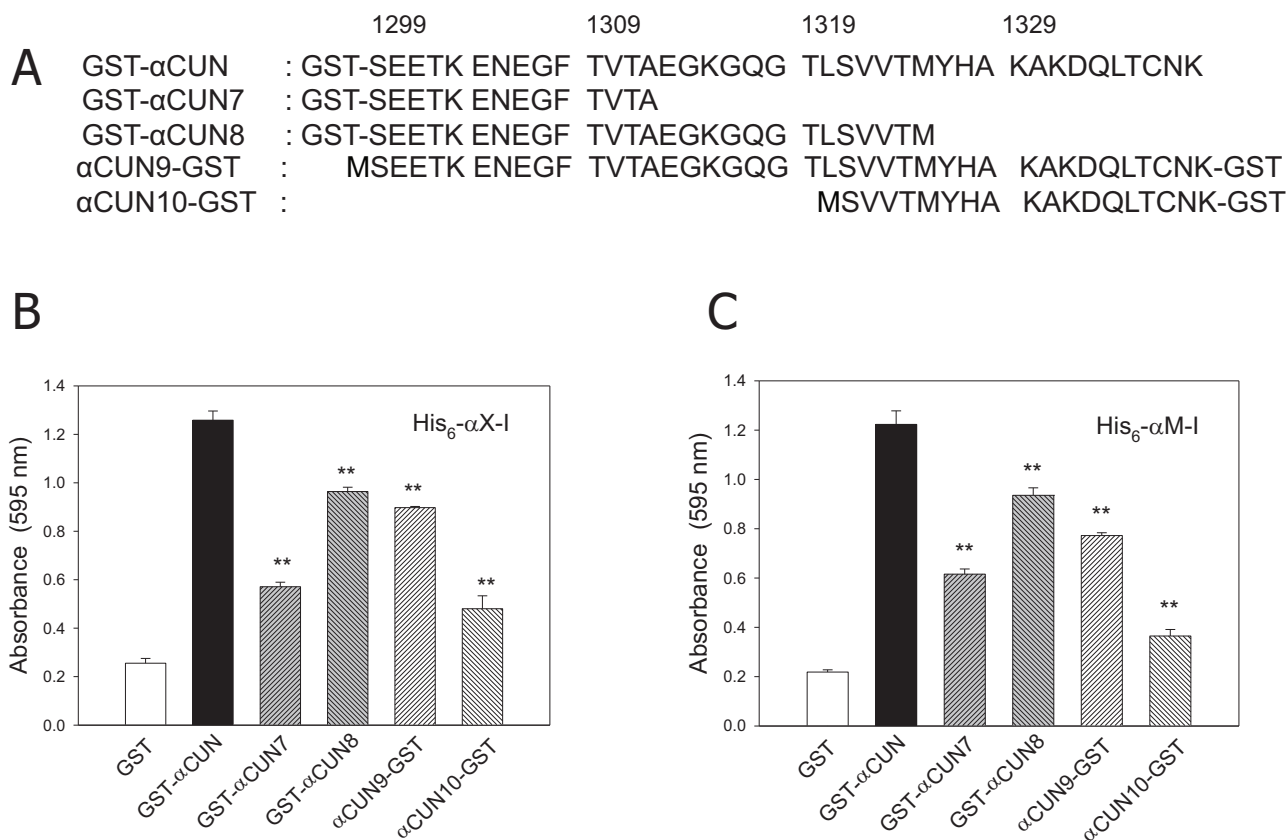

Fig. 5. Binding analyses of various CUN polypeptides to αX and αM I-domains. (A) Amino acid sequences of various CUN polypeptide N- and C-terminal GST fusions. (B and C) ELISA-based binding analyses of the CUN polypeptides αX and αM I-domains. The C-terminal of GST fusion peptides (αCUN, αCUN7, and αCUN8) and N-terminal of GST fusion peptides (αCUN9 and αCUN10) were loaded onto ELISA plate wells coated with the His$_6$-αX I-domain (B) or the His$_6$-αM I-domain (C). Results for each αCUN fusion variants (1 μM) are shown as mean ± SD (n = 3). **$P < 0.01$ for the comparison of mutant to wild type GST-αCUN binding.

peptide mutants binding to isolated αX I-domain largely mirror the results obtained with mutant iC3b binding to intact αMβ2 on activated neutrophils and confirm the important role of the acidic residues within the α'NT segment in the binding interaction with both αMβ2 and αXβ2.

The nature of αCUN binding to the I-domain of β2 integrin

To further localize the segments within αCUN contributing to its binding to the αX I-domain, various truncated mutants of both the N- and C-terminal αCUN GST fusions (nomenclature key in Fig. 5A) were purified and tested for their binding activities in an ELISA-based assay. As shown in Fig. 5B, the binding activities of the αCUN polypeptide segments fused to the GST C-terminus (GST-αCUN, GST-αCUN7, GST-αCUN8) are related to the length of the chain. However, in the case of the peptide segments fused to the N-terminus of GST, αCUN9-GST shows a slightly lower level of binding despite it having the same length of the CUBf-derived peptide as GST-αCUN. This may reflect differences in the accessibility of the CUBf-derived peptide segment when it is an N-terminal or C-terminal fusion of GST, or it may be that having an N-terminal Met residue is somewhat inhibitory to the binding of the peptide segment to the αX I-domain. Regardless of whether the test species is an N- or C-terminal fusion of GST, the shorter chain derivatives (αCUN7 and αCUN10) still

show above background binding activity to the αX I-domain, suggesting multiple binding sites dispersed along the length of the αCUN polypeptide segment. This binding pattern suggesting multiple binding sites for the αX I-domain can also be observed in αM I-domain. (Fig. 5C). This notion is consistent with the previous SPR data on peptide binding (Figs. 3D and 3E), showing that two discrete peptides (SEETKENE and TAE-GKGQG) were active in binding to αX I-domain.

As a cluster of acidic amino acids close to the N-terminus were found to be critical for the binding of αNTN, we decided to determine whether this was also true for the αCUN. Three mutants of αCUN with alanine substitution of acidic amino acids (depicted in Fig. 6A) were tested for their binding activities. The results of the ELISA-based assay show that point mutations at E1304, E1306 (αCUN5) and E1313 (αCUN6) reduce the binding activity of αCUN to both the αX and αM I-domains, whereas alanine mutations at E1300 and E1301 (αCUN4), if anything, have a small enhancing effect on the binding (Fig. 6B). In an SPR experiment measuring binding level to a CM5 chip-immobilized αXI-domain, both αCUN5 and αCUN6 bound more poorly than did the parent αCUN molecule (Figs. 6C and 6D). Also, consistent with the somewhat enhanced binding seen for αCUN4 in the ELISA-based binding assay, the SPR experiment suggests a decreased dissociation rate for this variant (Fig. 6C). Thus, like the situation in the α'NT segment, acidic residues play an important
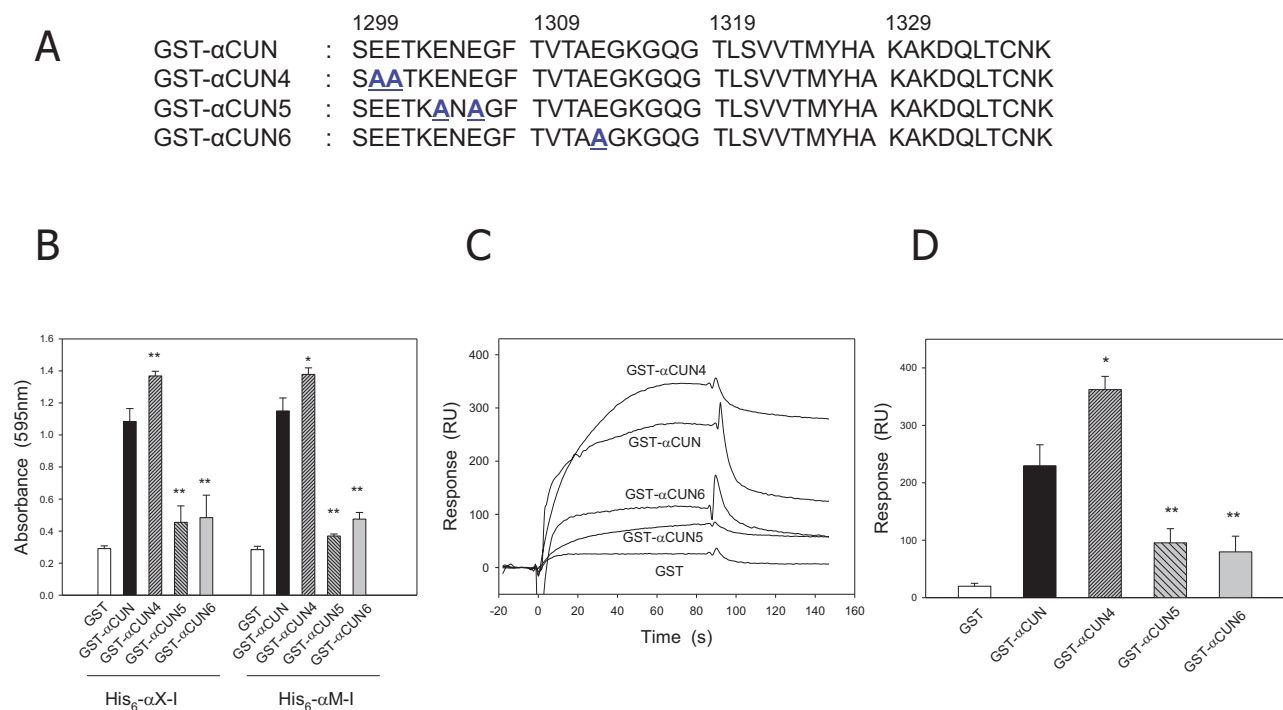

		1299	1309	1319	1329
GST-αCUN	:	SEETKENEGF	TVTAEGKGQG	TLSVVTMYHA	KAKDQLTCNK
GST-αCUN4	:	S**AA**TKENEGF	TVTAEGKGQG	TLSVVTMYHA	KAKDQLTCNK
GST-αCUN5	:	SEETK**A**N**A**GF	TVTAEGKGQG	TLSVVTMYHA	KAKDQLTCNK
GST-αCUN6	:	SEETKENEGF	TVTA**A**GKGQG	TLSVVTMYHA	KAKDQLTCNK

Fig. 6. Binding analyses of wild type and mutant GST-αCUN variants to the αX and αM I-domains. (A) Amino acid sequences of wild type GST-αCUN and its alanine substitution mutants (acidic residues to alanine denoted in underbars). (B) An ELISA-based binding assay of GST-αCUN and its mutants (1 μM) to the αX and αM I-domains. Results are shown as mean ± SD (n = 3). *$P < 0.05$, **$P < 0.01$ for the comparison of mutant to wild type GST-αCUN binding. (C) SPR sensograms of GST-αCUN and its mutants (1 μM each) binding to biosensor chip-immobilized His$_6$-αX-I (3800 RU). (D) Binding activities of the mutant GST-αCUN variants to αX I-domain. Each variant binding level was measured from the steady-state plateau region of their respective SPR sensograms. Data is shown as mean ± SD (n = 3). *$P < 0.05$, **$P < 0.01$.
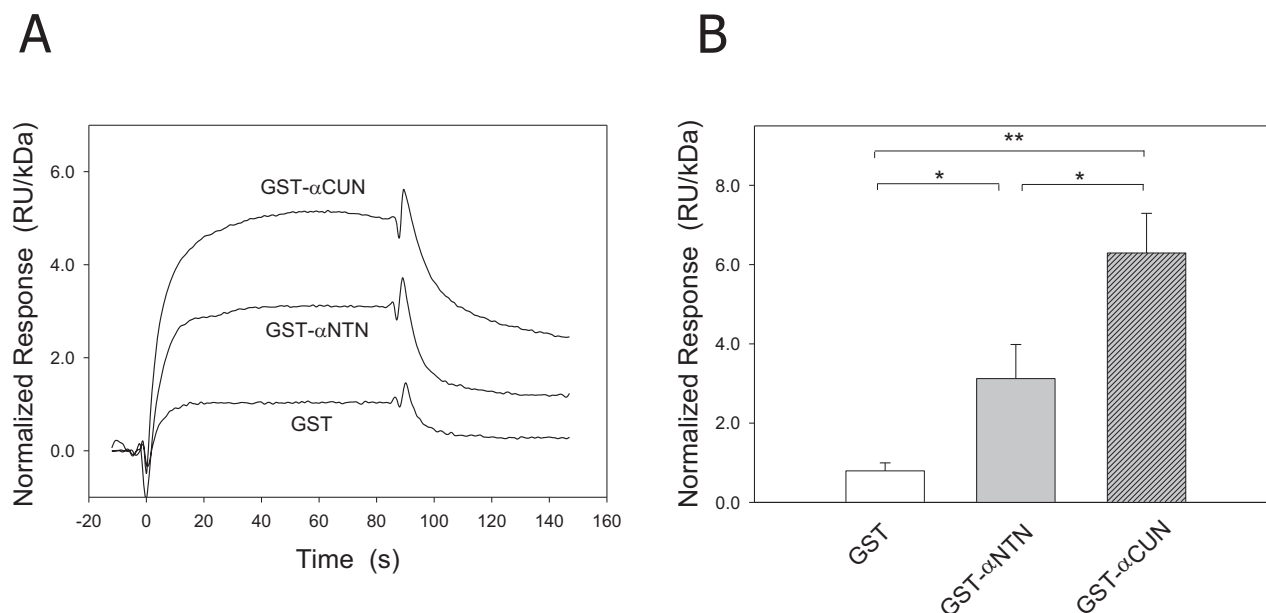
A

B

Fig. 7. Relative binding activities of GST-αNTN and GST-αCUN to αX I-domain. (A) SPR sensograms showing the relative binding activities of GST-αNTN, GST-αCUN and GST (1 μM each) to immobilized His₆-αX I-domain (3800 RU). Since in SPR the signal is proportional to the mass of the analyte bound to the biosensor chip, the raw RU results were normalized for differences in molecular mass and reported as RU/kDa. (B) Comparison of binding activities of GST-αNTN and GST-αCUN. The maximum RU of each protein was measured from the steady-state plateau region of their respective SPR sensograms. Data is shown as mean ± SD (n = 3). $*P < 0.05$, $**P < 0.01$.

role in the I-domain binding interaction with the N-terminal segment of CUBf, although in this case the N-terminal-most pair of acidic residues appear to play a more secondary role of modulation in the binding interaction.

The previous result of this study (Fig. 3B) suggests that the binding affinity of the αX I-domain for GST-αCUN appears to be several times higher than that for GST-αNTN. To compare the relative binding strengths of GST-αNTN and GST-αCUN for the I-domain, an SPR experiment was carried out. The results of the SPR sensograms have been normalized for differences in the molecular masses of the analytes. As shown in Fig. 7, GST-αCUN shows about a two-fold higher binding activity to the αX-I domain than GST-αNTN.

DISCUSSION

Complement fragment iC3b serves as the major opsonin for facilitating phagocytosis by CR4/αXβ2 on tissue resident macrophages. In this study, we have advanced our understanding of the molecular nature of this interaction through the delineation of three moieties within iC3b contributing to the interaction with the αX I-domain. Specifically, we have provided evidence for the involvement of both α'NT, the C3 convertase-generated N-terminal segment of the C3 α'-chain, and CUBf segment, a segment encompassing the FI-generated N-terminus in the CUBf region of the C3 α-chain produced during the C3b to iC3b conversion. In addition to our main focus on the binding moieties of iC3b for the αX I-domain, we found that the CUBf segment can be one of the regions of iC3b recognized by αMβ2.

Integrin αXβ2 has been characterized as a danger receptor, which recognizes negatively charged regions of proteolyzed and denatured proteins (Vorup-Jensen et al., 2005). A number of years ago, recognizing the abundance of negatively charged side chains in both the α'NT and the FI-cleavage-generated N-terminus of CUBf, we formulated the hypothesis that conformational events of C3 precipitated by protease cleavage can reveal previously cryptic sites near the new N-termini, and that these would participate in the binding of iC3b to αXβ2 integrin, and specifically to its I-domain.

Our experimental findings regarding the importance of acidic residues within the α'NT and N-terminal CUBf peptide segments in mediating their binding to the αX I-domain was not only consistent with our hypothesis, but can now be interpreted more fully in light of more recent negative stain EM image-derived structural information in the literature regarding the modes of binding of αX I-domain to iC3b (Xu et al., 2017). Specifically, it was revealed that either as an isolated αX I-domain, or within the context of the intact extracellular headpiece portion αXβ2 heterodimer, there are actually two independent sites through which a single iC3b molecule may bind the αX I-domain. One of these sites is in the β-chain ring at the interface between domains MG3 and MG4, whereas the other is near the C345C domain at the "top" of the molecule, putting it in the vicinity of the two segments identified here, as binding to αX I-domain. The α'NT segment lies across the MG7 domain just below the C345C domain (Fig. 1A), the latter being visualized as a distinct knob in the EM images and thereby facilitating identification of the area contacted by the αX I-domain. The factor I cleavage-generated CUBf

segment extends the N-terminal from the MG8 domain and, based on a structural study employing hydrogen-deuterium exchange mass spectroscopy of iC3b, this segment is suggested to have a high structural flexibility (Papanastasiou et al., 2017), and thus could easily reside on the same side of the molecule as the α'NT segment. Accordingly, both of these acidic residue-rich segments could simultaneously engage with a positively charged face of the αX I-domain. Indeed, Xu et al. (2017) had speculated upon the SEETKENEG peptide segment at the N-terminus of the residual CUBf domain as a potential candidate site for facilitating this binding, a point which we have now provided direct experimental evidence for. As an aside, the MG3-MG4 interface is also quite negatively charged, so the involvement of the same face of the I-domain to this binding site of iC3b is also possible.

The potential for charge complementarity appears to be a common thread on both sides of the iC3b:I-domain interface throughout the studies we report here. The α'NT and the CUBf segment of iC3b that our results implicate in binding to the αM and αX I-domains share the common feature of being acidic residue rich. The basic residues, K242 and K243 of the βDα5 loop at the "top" of the αX I-domain, which we show are vital for iC3b binding, are part of a basic groove spanning the MIDAS surface of the molecule (Vorup-Jensen et al., 2003). In a structural study of the αM I-domain liganded by C3d, it was shown that the D1245 of C3d engages in an ionic interaction with the R208 of αM I-domain (Bajic et al., 2013). This result reinforces our notion of the charge complementarity on the binding of iC3b to the αM and αX I-domains. However, this is not to say that only ionic interactions are important for the binding, as other residues on the same face of the αM I-domain, including Q204, L205, T211, T213, I256, and P257, all of which are conserved between the αM and the αX I-domains, have been suggested as contributing to the binding of iC3b to the αM I-domain (Ustinov and Plow, 2005). With a direct structural comparison of the electrostatic charges in the MIDAS of the αM and αX I-domain, it is notable that the αX I-domain presents a ridge of positively charged residues which are not found in the αM I-domain. For example, K242 in αX is substituted by E244 in αM, which results in a disruption of the positively-charged groove on the MIDAS-containing "top" face of αM I-domain (Vorup-Jensen and Jensen, 2018). It is therefore tempting to speculate that relative to the robust binding seen for the αX I-domain, the weaker binding displayed by the αM I-domain, not only for intact iC3b, but also for its α'NT and CUBf segment, is at least partially due to this loss in potential charge complementarity between the binding entities.

It is possible that there still exist unidentified moieties of iC3b involved in binding to the αM and αX I-domains besides the sites reported in this study. Ultimately, a high resolution structure of iC3b in complex with an αX I-domain may be achieved that can potentially reveal the nature of the interface in atomic detail. Our characterization of the two distinct binding moieties within iC3b for the I-domain of the αX integrin will provide the necessary foundation for a detailed understanding of this crucial interface involved in mediating phagocytic clearance of complement-opsonized pathogens.

AUTHOR CONTRIBUTIONS
S.-U.N. designed all the experiments and wrote the manuscript. J.C. and D.B. performed the experiments.

CONFLICT OF INTEREST
The authors have no potential conflicts of interest to disclose.

ORCID
Jeongsuk Choi   https://orcid.org/0000-0003-3351-131X
Sang-Uk Nham   https://orcid.org/0000-0001-7854-759X

REFERENCES

Arnaout, M.A., Mahalingam, B., and Xiong, J.P. (2005). Integrin structure, allostery, and bidirectional signaling. Annu. Rev. Cell Dev. Biol. *21*, 381-410.

Bajic, G., Yatime, L., Sim, R.B., Vorup-Jensen, T., and Andersen, G.R. (2013). Structural insight on the recognition of surface-bound opsonins by the integrin I domain of complement receptor 3. Proc. Natl. Acad. Sci. U. S. A. *110*, 16426-16431.

Becherer, J.D., Alsenz, J., Esparza, I., Hack, C.E., and Lambris, J.D. (1992). Segment spanning residues 727-768 of the complement C3 sequence contains a neoantigenic site and accommodates the binding of CR1, factor H, and factor B. Biochemistry *31*, 1787-1794.

Carroll, M.C. (2004). The complement system in regulation of adaptive immunity. Nat. Immunol. *5*, 981-986.

Choi, J., Choi, J., and Nham, S.U. (2010). Characterization of the residues of αX I-domain and ICAM-1 mediating their interactions. Mol. Cells *30*, 227-234.

Diamond, M.S., Garcia-Aguilar, J., Bickford, J.K., Corbi, A.L., and Springer, T.A. (1993). The I domain is a major recognition site on the leukocyte integrin Mac-1 (CD11b/CD18) for four distinct adhesion ligands. J. Cell Biol. *120*, 1031-1043.

Gaither, T.A., Vargas, I., Inada, S., and Frank, M.M. (1987). The complement fragment C3d facilitates phagocytosis by monocytes. Immunology *62*, 405-411.

Gang, J., Choi, J., Lee, J.H., and Nham, S.U. (2007). Identification of critical residues for plasminogen binding by the αX I-domain of the β2 integrin, αXβ2. Mol. Cells *24*, 240-246.

Gros, P., Milder, F.J., and Janssen, B.J. (2008). Complement driven by conformational changes. Nat. Rev. Immunol. *8*, 48-58.

Helmy, K.Y., Katschke, K.J., Gorgani, N.N., Kljavin, N.M., Elliott, J.M., Diehl, L., Scales, S.J., Ghilardi, N., and van Lookeren Campagne, M. (2006). CRIg: a macrophage complement receptor required for phagocytosis of circulating pathogens. Cell *124*, 915-927.

Inada, S., Brown, E.J., Gaither, T.A., Hammer, C.H., Takahashi, T., and Frank, M.M. (1983). C3d receptors are expressed on human monocytes after in vitro cultivation. Proc. Natl. Acad. Sci. U. S. A. *80*, 2351-2355.

Janssen, B.J. and Gros, P. (2007). Structural insights into the central complement component C3. Mol. Immunol. *44*, 3-10.

Janssen, B.J., Huizinga, E.G., Raaijmakers, H.C., Roos, A., Daha, M.R.,

Nilsson-Ekdahl, K., Nilsson, B., and Gros, P. (2005). Structures of complement component C3 provide insights into the function and evolution of immunity. Nature *437*, 505-511.

Lee, J.H., Choi, J., and Nham, S.U. (2007). Critical residues of αX I-domain recognizing fibrinogen central domain. Biochem. Biophys. Res. Commun. *355*, 1058-1063.

Lee, J.O., Rieu, P., Arnaout, M.A., and Liddington, R. (1995). Crystal structure of the A domain from the alpha subunit of integrin CR3 (CD11b/CD18). Cell *80*, 631-638.

Luo, B.H., Carman, C.V., and Springer, T.A. (2007). Structural basis of integrin regulation and signaling. Annu. Rev. Immunol. *25*, 619-647.

Michishita, M., Videm, V., and Arnaout, M.A. (1993). A novel divalent cation-binding site in the A domain of the β2 integrin CR3 (CD11b/CD18) is essential for ligand binding. Cell *72*, 857-867.

Myones, B.L., Dalzell, J.G., Hogg, N., and Ross, G.D. (1988). Neutrophil and monocyte cell surface p150,95 has iC3b-receptor (CR4) activity resembling CR3. J. Clin. Invest. *82*, 640-651.

Papanastasiou, P., Koutsogiannaki, S., Sarigiannis, Y., Geisbrecht, B.V., Ricklin, D., and Lambris, J.D. (2017). Structural implications for the formation and function of the complement effector protein iC3b. J. Immunol. *198*, 3326-3335.

Pettersen, E.F., Goddard, T.D., Huang, C.C., Couch, G.S., Greenblatt, D.M., Meng, E.C., and Ferrin, T.E. (2004). UCSF Chimera-a visualization system for exploratory research and analysis. J. Comput. Chem. *25*, 1605-1612.

Plow, E.F., Haas, T.A., Zhang, L., Loftus, J., and Smith, J.W. (2000). Ligand binding to integrins. J. Biol. Chem. *275*, 21785-21788.

Ricklin, D., Hajishengallis, G., Yang, K., and Lambris, J.D. (2010). Complement: a key system for immune surveillance and homeostasis. Nat. Immunol. *11*, 785-797.

Ross, G.D. and Medof, M.E. (1985). Membrane complement receptors specific for bound fragments of C3. Adv. Immunol. *37*, 217-267.

Taniguchi-Sidle, A. and Isenman, D.E. (1992). Mutagenesis of the Arg-Gly-Asp triplet in human complement component C3 does not abolish binding of iC3b to the leukocyte integrin complement receptor type III (CR*3*, CD11b/CD18). J. Biol. Chem. *267*, 635-643.

Taniguchi-Sidle, A. and Isenman, D.E. (1994). Interactions of human complement component C3 with factor B and with complement receptors type 1 (CR*1*, CD35) and type 3 (CR*3*, CD11b/CD18) involve an acidic sequence at the N-terminus of C3 α'-chain. J. Immunol. *153*, 5285-5302.

Ueda, T., Rieu, P., Brayer, J., and Arnaout, M.A. (1994). Identification of the complement iC3b binding site in the β2 integrin CR3 (CD11b/CD18). Proc. Natl. Acad. Sci. U. S. A. *91*, 10680-10684.

Ustinov, V.A. and Plow, E.F. (2005). Identity of the amino acid residues involved in C3bi binding to the I-domain supports a mosaic model to explain the broad ligand repertoire of integrin αMβ2. Biochemistry *44*, 4357-4364.

Vorup-Jensen, T., Carman, C.V., Shimaoka, M., Schuck, P., Svitel, J., and Springer, T.A. (2005). Exposure of acidic residues as a danger signal for recognition of fibrinogen and other macromolecules by integrin αXβ2. Proc. Natl. Acad. Sci. U. S. A. *102*, 1614-1619.

Vorup-Jensen, T. and Jensen, R.K. (2018). Structural immunology of complement receptors 3 and 4. Front. Immunol. *9*, 1-20.

Vorup-Jensen, T., Ostermeier, C., Shimaoka, M., Hommel, U., and Springer, T.A. (2003). Structure and allosteric regulation of the αXβ2 integrin I domain. Proc. Natl. Acad. Sci. U. S. A. *100*, 1873-1878.

Xu, S., Wang, J., Wang, J.H., and Springer, T.A. (2017). Distinct recognition of complement iC3b by integrins αXβ2 and αMβ2. Proc. Natl. Acad. Sci. U. S. A. *114*, 3403-3408.